

Detection of Heavy Metal Ions in Water by High-Resolution Surface Plasmon Resonance Spectroscopy Combined with Anodic Stripping Voltammetry

Shaopeng Wang,^{*,†} Erica S. Forzani,[‡] and Nongjian Tao[‡]

Nomadics, Incorporated, Stillwater, Oklahoma 74074, and Department of Electrical Engineering, Arizona State University, Tempe, Arizona 85287

High-resolution differential surface plasmon resonance (SPR) with anodic stripping voltammetry (ASV) capability has been demonstrated for detecting heavy metal ions in water. Metal ions are electroplated onto the gold SPR sensing surface and are quantitatively detected by stripping voltammetry. Both the SPR angular shift and electrochemical current signal are recorded to identify the type and amount of the metal ions in water. The performance of the combined approach is further enhanced by a differential detection approach. The gold sensor surface is divided into a reference and a sensing area, and the difference in the SPR angles from the two areas is detected with a quadrant cell photodetector as a differential signal. Our system demonstrated quantitative detection of copper, lead, and mercury ions in water from part-per-million to sub-part-per-billion levels with good linearity.

Heavy metal poisoning due to contamination of groundwater, surface water, and soil has been a serious concern in many areas of the globe. The current method for detection of heavy metal ions in water and other matrices still largely relies on sending a technician to the field, collecting samples, and bringing them to a laboratory for analysis. This approach is not only time-consuming and inconvenient but also expensive and prone to errors that may occur during sample transportation and handling. A number of portable devices have been developed, which include anodic stripping voltammetry (ASV),^{1–3} X-ray fluorescence,⁴ and immunoassay-based detection kits. These devices are not widely used due to various technical or other limitations. A low-cost, easy-to-use, and reliable device is still much needed for environmental monitoring and analysis. Such a device could also be used in medical diagnostics for early detection of heavy metal poisoning

in children, which is especially important in developing countries.

ASV is an established technology for sensitive and selective detection of metal ions and other electrochemically active substances.^{1,2} However, ASV has several limitations. First, the sample must be dissolved in supporting electrolyte. Second, ASV often uses mercury as the working electrode, which is not environmentally friendly. Third, the presence of background current in ASV measurement makes it difficult to detect the small stripping current associated with the oxidation of the analytes. Finally, ASV measures only redox-active species and processes, and the formation of intermetallic compounds between two different metals can disturb the individual stripping peaks.

Surface plasmon resonance spectroscopy (SPR) is a sensitive method for detecting analytes adsorbed on a metal surface.⁵ It has been widely used as a biomedical and pharmaceutical research tool to screen biological and chemical analytes.⁶ Surface plasmons are collective oscillations of free electrons in a metallic film. Under an appropriate condition, the plasmons can resonate with an incident light beam and absorb the energy of the beam.^{7,8} Because the resonance condition is extremely sensitive to the refractive index of the medium adjacent to the metallic film, the presence of molecules on the surface of the metallic film can be accurately detected. Efforts to combine SPR with ASV techniques have been reported for metal ion detection.^{9–12} These pioneering experiments showed that SPR measurement is insensitive to background current, such as background current introduced by dissolved oxygen,¹³ a limiting source in ASV measurements. Another advantage of SPR measurement is its sensitivity to solid reaction products such as intermetallic compounds, which are not detectable by ASV. However, the SPR detection of metal ions in the previous experiments is less sensitive than ASV.

* To whom correspondence should be addressed. E-mail: swang@nomadics.com. Phone: (405) 372-9535. Fax: (405) 372-9537.

[†] Nomadics, Incorporated.

[‡] Arizona State University.

(1) Wang, J. *Stripping Analysis: Principles, Instrumentation, and Applications*; VCH Publishers: Deerfield Beach, FL, 1985.

(2) Wang, J. *New Approaches to Metal Speciation in Natural Waters Based on Modified and Microvoltammetric Electrodes*; Summary Report 251; Department of Chemistry, New Mexico State University: La Cruces, NM, 1990.

(3) Barbeira, P. J. S.; Stradiotto, N. R. *Fresenius' J. Anal. Chem.* **1998**, 361, 507–509.

(4) Klockenkamper, R.; Bohlen, A. v. *X-Ray Spectrom.* **1996**, 25, 156–162.

(5) Homola, J.; Yee, S. S.; Gauglitz, G. *Sens. Actuators, B* **1999**, 54, 3–15.

(6) Myszk, D. G. *J. Mol. Recognit.* **1999**, 12, 390–408.

(7) Otto, A. Z. *Phys.* **1968**, 216, 398–407.

(8) Kretschmann, E. Z. *Phys.* **1971**, 241, 313–324.

(9) Chinowsky, T. M.; Saban, S. B.; Yee, S. S. *Sens. Actuators, B* **1996**, 35–36, 37–43.

(10) Yee, S. S.; Jung, C. C.; Saban, S. B.; Darling, R. B. U.S. Patent 5858799, 1999.

(11) Jung, C. C.; Saban, S. B.; Yee, S. S.; Darling, R. B. *Sens. Actuators, B* **1996**, 32, 143–147.

(12) Mirkhalaf, F.; Schifffrin, D. J. *J. Electroanal. Chem.* **2000**, 484, 182–188.

(13) Iwasaki, Y.; Horiuchi, T.; Morita, M.; Niwa, O. *Sens. Actuators, B* **1998**, 50, 145–148.

We have recently reported on a simple SPR sensor that achieves high resolution ($\sim 10^{-5}$ deg) by using a bicell or a quadrant cell photodetector.^{14–23} The use of quadrant cell detection further minimizes the undesired effects due to mechanical vibrations and thermal drifts, as well as the influence of the refractive index changes in the bulk solution. These experiments have demonstrated selective detection of Cu^{2+} and Ni^{2+} ions in the part-per-billion to part-per-trillion range by using highly selective peptides as molecular recognition elements.¹⁷ However, this approach is limited by the fact that many toxic metal ions do not have a specific probe.

In this paper, we report a combined high-resolution differential SPR and ASV approach to analyze trace metal ions in water. We have demonstrated detection of lead, copper, and mercury ranging from sub-part-per-billion to part-per-million levels. The system can be developed into a portable device for monitoring trace metal ions in drinking water, wastewater, and groundwater and for rapid screening of toxic metal ions or other electrochemically active species in blood, saliva, and urine.

EXPERIMENTAL DETAILS

Chemicals and Sample Preparation. All chemicals were purchased from Sigma-Aldrich with analytical or HPLC grade and used without further purification. $\text{Pb}(\text{NO}_3)_2$, $\text{Cu}(\text{NO}_3)_2$, and $\text{Hg}(\text{ClO}_4)_2$ were dissolved or diluted to different concentrations of Pb^{2+} , Cu^{2+} , and Hg^{2+} sample solution with the selected electrolyte solutions: 0.1 M HClO_4 , 0.1 M NaClO_4 , or 10 mM Tris–HCl buffer pH 5.

Instrumentation. The bicell and quadrant cell SPR setups are similar to the previously described systems.^{14–16,18,23} Figure 1 shows the schematics of the quadrant cell SPR–ASV system. The photocurrents from the four cells (A, B and C, D) of quadrant cell photodetector were converted to voltages with a homemade circuit. The circuit calculate $A - B$, $A + B$, $C - D$, and $C + D$, where $(A - B)/(A + B)$ and $(C - D)/(C + D)$ are linearly proportional to the SPR angular shift of the sample and the reference channel, respectively. The circuit also has analog dividers that calculate $(A - B)/(A + B) - (C - D)/(C + D)$, which gives the differential signal that measures the difference of the SPR angle shift between the two channels. The detector is mounted on a precision X–Y translation stage (Parker Hannifin, model 3946), and the X–Y stage is mounted on a precise rotational stage (Newport RS65). This combined translational and rotational control was used to bring both $A - B$ and $C - D$ close to zero

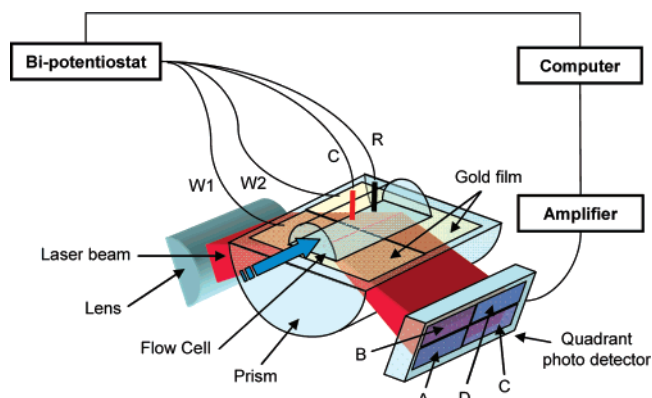


Figure 1. Diagram of a quadrant cell differential SPR metal ion sensor. W1 and W2 are the sampling and reference areas, C is a counter electrode, and R is a reference electrode, respectively.

before each experiment. A 12-bit National Instruments AD/DA board (PCI 6071) was used to collect the SPR and electrochemical signal (potential and current of the sample and reference channels).

Sample solutions were introduced into the system using either a static or a flow sample cell. The gold surface was cut in the center (Figure 1) to make two insulated working electrode areas, representing the sample and the reference channel. A platinum wire (diameter of 0.1 mm) and a thin platinum sheet were used as the counter electrode for the static cell and flow cell, respectively. A Ag/AgCl nonleak electrode from Cypress Systems (www.cypresssystems.com) was used as a reference electrode for both the static and flow cells. A bipotentiostat (Pine, AFCBP1) was used for potential control and electrochemical measurements. The volume of the static cell is about 0.5 mL, and the surface area of the gold film exposed to the sample is about 30 mm². In the case of the flow cell, the volume is 5 μL with an effective gold film surface area of 8 mm². A syringe pump (Yale Apparatus, YA-12) with a programmable flow rate and volume was used for sample injection. The potential sweep can be either controlled from the potentiostat or a computer. The control and data collection software was programmed with LabView for Windows. The angular resolution of the differential signal is 10^{-5} deg, and the overnight drift is less than 10^{-3} deg, as shown in Figure S-1 (in the Supporting Information).

For bicell detections, the quadrant cell was replaced with a bicell photodetector to measure the $A - B$ and $A + B$ signals. The gold sensing surface for the bicell system was used as a single working electrode. A silver wire was used as the reference electrode for the bicell system.

SPR–ASV Detection Process. Before each measurement, a blank buffer was first loaded in the sample cell (static or flow cell) and the prism was positioned so that there was a dark line located near the center of the reflected laser beam. The dark line was due to the absorption of the light by the surface plasmon, which occurs at the angle of resonance. The reflected light falling onto the photodetector was then centered by adjusting the photodetector position with the translation stage until $A - B$ and $C - D$ approached zero. Next, the sample to be measured was introduced into the sample cell to replace the blank buffer and a negative potential, lower than the Nernst potentials of the metal ions to be measured, was applied to the gold surface (working electrode S)

- (14) Boussaad, S.; Huang, W. L.; Tao, N. J. *International Patent* WO00070328, 2000.
- (15) Boussaad, S.; Pean, J.; Tao, N. J. *Anal. Chem.* **2000**, *72*, 222–226.
- (16) Boussaad, S.; Tao, N. J. *J. Electroanal. Chem.* **2003**, *554*, 233–239.
- (17) Forzani, E. S.; Zhang, H. Q.; Chen, W.; Tao, N. J. *Environ. Sci. Technol.* **2005**, *39*, 1257–1262.
- (18) Song, F. Y.; Zhou, F. M.; Wang, J.; Tao, N. J.; Lin, J. Q.; Vellanoeth, R. L.; Morquecho, Y.; Wheeler-Laidman, J. *Nucleic Acids Res.* **2002**, *30*, e72/1–e72/11.
- (19) Tao, N. J.; Boussaad, S.; Huang, W. L.; Arechabaleta, R. A.; D'Agnese, J. *Rev. Sci. Instrum.* **1999**, *70*, 4656–4660.
- (20) Wang, S.; Boussaad, S.; Tao, N. J. *Rev. Sci. Instrum.* **2001**, *72*, 3055–3060.
- (21) Wang, S.; Boussaad, S.; Wang, S.; Tao, N. J. *Anal. Chem.* **2000**, *72*, 4003–4008.
- (22) Yao, X.; Wang, J. X.; Zhou, F. M.; Wang, J.; Tao, N. J. *J. Phys. Chem. B* **2004**, *108*, 7206–7212.
- (23) Zhang, H. Q.; Boussaad, S.; Tao, N. J. *Rev. Sci. Instrum.* **2003**, *74*, 150–153.

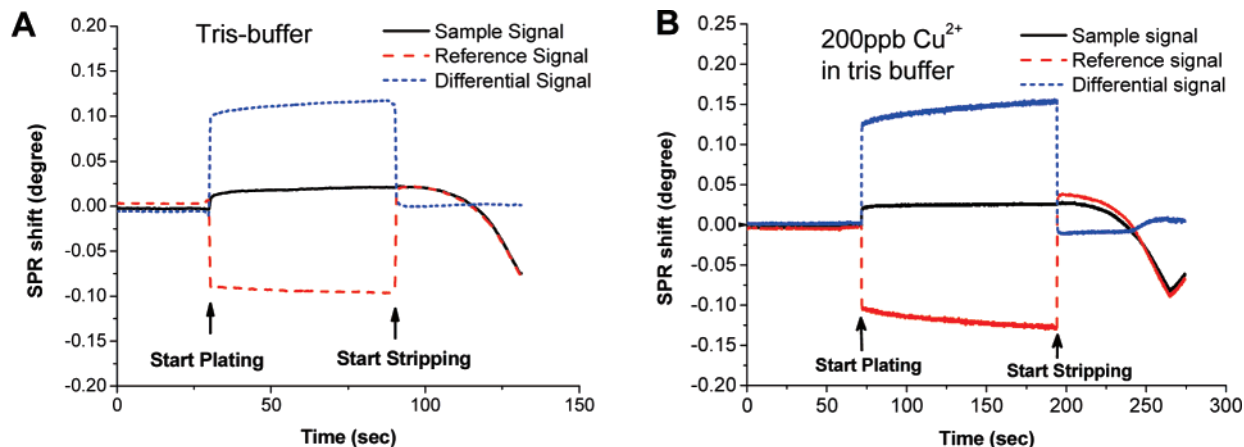


Figure 2. Quadrant cell SPR-ASV measurement processes: plating and stripping. The sample, reference, and differential SPR signals are plotted vs time. (A) The sample was 10 mM Tris-HCl buffer pH 5. The plating voltages for the sample and reference channel were -0.4 and 0.4 V, respectively. At the end of the plating period, the voltage of the reference channel drops to -0.4 V, and both channels are stripped to 0.4 V at a sweep rate of 20 mV/s. (B) The sample was 200 ppb Cu^{2+} in 10 mM Tris-HCl buffer pH 5. The plating voltages for the sample and reference channel were -0.7 and 0.7 V, respectively. At the end of the plating period, the voltage of the reference channel drops to -0.7 V, and both channels are stripped to 0.7 V at a sweep rate of 20 mV/s.

for a given time. The metal ions to be measured were reduced and plated on the gold surface. During this process, the SPR angle shifted by an amount proportional to the amount of metal ions plated on the surface. The potential of the reference channel was maintained at a positive potential to prevent the metal plating from taking place. The plating time was selected based on the concentration range of the analytes and the sample volume. In the case of the flow cell, a higher flow rate can reduce the plating time necessary to obtain the same level of signal. At the end of the plating period, the reference channel was brought to the same negative potential as the sample channel, and the potentials of both channels were immediately swept positively and stopped at a potential higher than the highest oxidization potential of the metal. During this positive potential sweep, the metal plated on the sample channel was oxidized to the ionic form and stripped off. We note that because the reference channel was below the Nernst potential only very briefly, the amount of metal plated on the electrode of the reference channel is minimal. The difference in the SPR angle shifts between the two channels reflects the amount of metal deposited on the sample channel. This differential method is similar to subtractive ASV.¹ Interferences in the sample, such as organic residues and particles, were nonspecifically attached to both the sample and reference channels and were cancelled out with differential detection. The voltage-dependent SPR shift due to the capacitor effect was also cancelled out in the quadrant cell approach. In addition, the current signal was recorded as in subtractive ASV, and the peak area was proportional to the amount of the metal.

Figure 2 shows a measurement process of quadrant cell SPR-ASV detection of (Figure 2A) 10 mM Tris-HCl buffer and (Figure 2B) 200 ppb copper(II) in 10 mM Tris-HCl buffer. The copper was stripped off at about 0 V. The surface-charging effect gave potential-dependent SPR signal shifts on both the sampling and reference channels, regardless of the presence of copper ions. However, at the stripping step, both channels had the same potential applied, and the surface-charging effect was cancelled out in the differential signal. The differential SPR signal showed only a shift caused by the change of refractive index on the surface

due to the stripping of the metal. Depending on the dielectric properties of the metal, either a positive or a negative shift could occur. In the case of copper, the stripping caused a positive shift (to a higher SPR angle). The detection process of the bicell SPR-ASV system is the same as the sampling channel of the quadrant cell SPR, as shown in Supporting Information Figure S-2.

RESULTS AND DISCUSSION

Detection of Lead(II) with the Bicell SPR-ASV System.

Figure 3 shows the bicell SPR-ASV detection of lead(II) in 0.1 M NaClO_4 solution at different concentrations. The static cell with 0.4 mL of total sample volume was used. Plating time was 5 min and plating potential was -0.9 V. All the spectra are blank (5 min plating and then stripping of 0.1 M NaClO_4) subtracted, in order to correct the surface charge density-induced slope. The subtraction also cancels most of the background interferences that are caused by impurities in the electrolyte solution. Lead(II) is stripped off at about -0.4 V. The SPR signal showed a negative shift, and the current signal showed a peak at the stripping potential. A concentration of 1 ppb of lead(II) can be detected by both the SPR signal and the current signal. However, the current signal is generated from the entire gold surface area that is exposed to the sample solution (~ 2 mm²), while the SPR signal is generated from the laser focusing point only (less than 0.01 mm²). For the same surface area, the SPR signal is 2 orders of magnitude more sensitive than the current measurement. The inset in Figure 3 shows the calibration plot of SPR shift versus lead concentration. The SPR angular shift values were defined as the SPR angle difference between the potential of -0.6 and -0.3 V. The calibration plot shows a linear relationship ($R^2 = 0.99$) between SPR signal and lead concentration in the sample.

Simultaneous Detection of Two Metals. Figure 4 shows the bicell ASV detection of lead(II) and copper(II) at different concentrations in 0.1 M NaClO_4 , with a 5 min plating at -0.9 V. Lead(II) shows a negative shift at -0.4 V, while copper(II) shows a positive shift at 0.2 V. The shift of copper stripping potential from 0 V (when only copper present in the sample) may be due to solvent effect and lead/copper interaction. Supporting Informa-

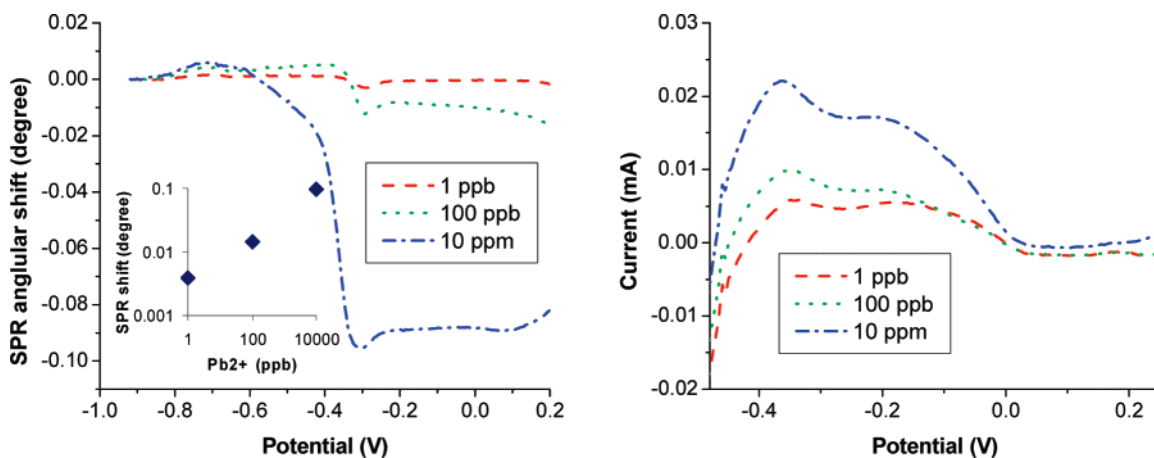


Figure 3. SPR (left) and current (right) stripping signal of different concentrations of Pb^{2+} in 0.1 M NaClO_4 . Both SPR and current signals were subtracted from the corresponding blank signal that was measured with a 0.1 M NaClO_4 solution at the same condition. Plating potential was -0.9 V and plating time was 5 min using a static cell with a sample volume of 0.4 mL. Inset in the left: SPR shift vs Pb^{2+} concentration. The SPR angular shift is the change in the SPR angle when the potential is changed between -0.6 and -0.3 V.

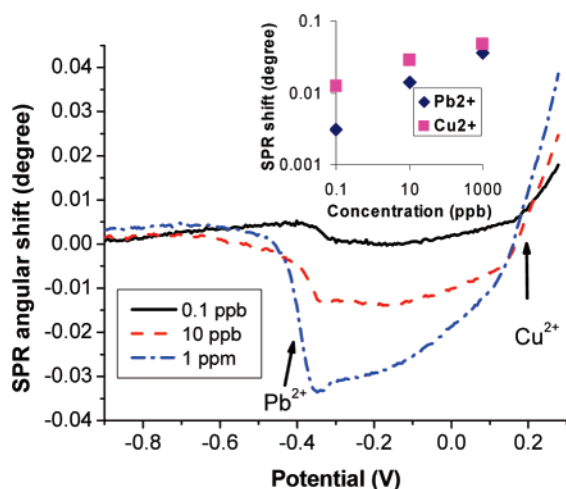


Figure 4. Simultaneous detection of different concentrations of Pb^{2+} and Cu^{2+} , with the bicell system. Pb^{2+} shows a negative shift at -0.4 V, and Cu^{2+} shows a positive shift at 0.2 V, in 0.1 M NaClO_4 . The data were collected holding the potential at -0.9 V for 5 min in a static cell. Inset: SPR shift vs Pb^{2+} and Cu^{2+} concentrations. The SPR angular shift is the difference in the SPR angles measured at -0.6 and -0.3 V for Pb^{2+} , and 0.25 and 0 V for Cu^{2+} , respectively.

tion Figure S-3 shows simultaneous detection of 100 ppb Cu^{2+} and Hg^{2+} , in 0.1 M HClO_4 . Copper shows a clear positive shift at 0.05 V, and Hg^{2+} shows a clear negative shift at 0.5 V. The reversed signals between copper and lead/mercury are due to the different refractive indices of the two metals and help to distinguish different metals especially when their stripping potentials are very close. The calibration plot (inset of Figure 4) shows that both metals retain close to linear relationship ($R^2 = 0.9$) on SPR signal versus metal concentration. We noted that the SPR signal of 0.1 ppb lead(II) in Figure 4 is larger than the SPR signal of 1 ppb lead(II) in Figure 3. This difference is most likely caused by interactions between copper and lead. Prado et al. has reported that deposited copper nuclei act as favorable sites for subsequent nucleation and growth of lead, and may increase the deposition rate of lead.²⁴

Detection of Mercury(II) with the Quadrant Cell SPR-ASV. Figure 5 shows the detection of different concentrations of $\text{Hg}(\text{II})$ in 0.1 M HClO_4 , with the quadrant cell system and the flow cell. The flow rate was 0.2 mL/min. The plating potential was 0 V, and a negative $\text{Hg}(\text{II})$ stripping shift appeared between 0.3 and 0.6 V. The SPR signals are shown in the left and the current signals are shown in the right side. The signal-to-noise ratio of the SPR signals is much higher than that of the current signals. The SPR angular shift has a close to linear relationship ($R^2 = 0.99$) with mercury concentration, and the 0.1 ppb mercury(II) gives a measurable SPR signal, as shown in the inset of Figure 5 (left). The baseline of the SPR signal may shift between measurements, due to the mechanical and electronic drift of the test system. But within the short time period of each measurement, the baseline is relatively stable, as shown in Supporting Information Figure S-1. In the inset of Figure 5, the SPR angular shift values were defined as the SPR angle difference between the potential at 0.2 and 0.8 V, which cancelled out the baseline drift between experiments. The current-voltage (CV) signal shows a kink at 0.3 V for up to 100 ppb $\text{Hg}(\text{II})$ and a peak at 0.6 V for 1 ppm $\text{Hg}(\text{II})$. The quadrant cell system measures the real-time differential signal and does not need a separate measurement on blank electrolyte and manual blank subtraction.

Plating Time and Flow Rate. Similar to the regular ASV measurement, the SPR signal strength is highly dependent on the plating time and the flow rate. Figure 6 shows the effect of flow rate and plating time on the detection of 100 ppb mercury(II). Both the higher flow rate and the longer plating time can increase signal level and improve the detection limit. For equal amounts of sample volume, a lower flow rate with a longer plating time gives a better signal. Both 0.5 mL/s flow rate with 200 s of plating and 0.1 mL/s flow rate with 1000 s of plating time give 1 mL sample volume, but the latter gives a doubled SPR signal level. This result indicates that the mercury in the sample is not fully deposited onto the gold electrode surface at high flow rates.

Surface Charge Density Effect. Changing of electrode potential is known to induce a change in the surface charge density of the electrode and cause a shift in the SPR angle.²¹ This charge density-induced SPR shift is approximately proportional

(24) Prado, C.; Wilkins, S. J.; Marken, F.; Compton, R. G. *Electroanalysis* 2002, 14, 262–272.

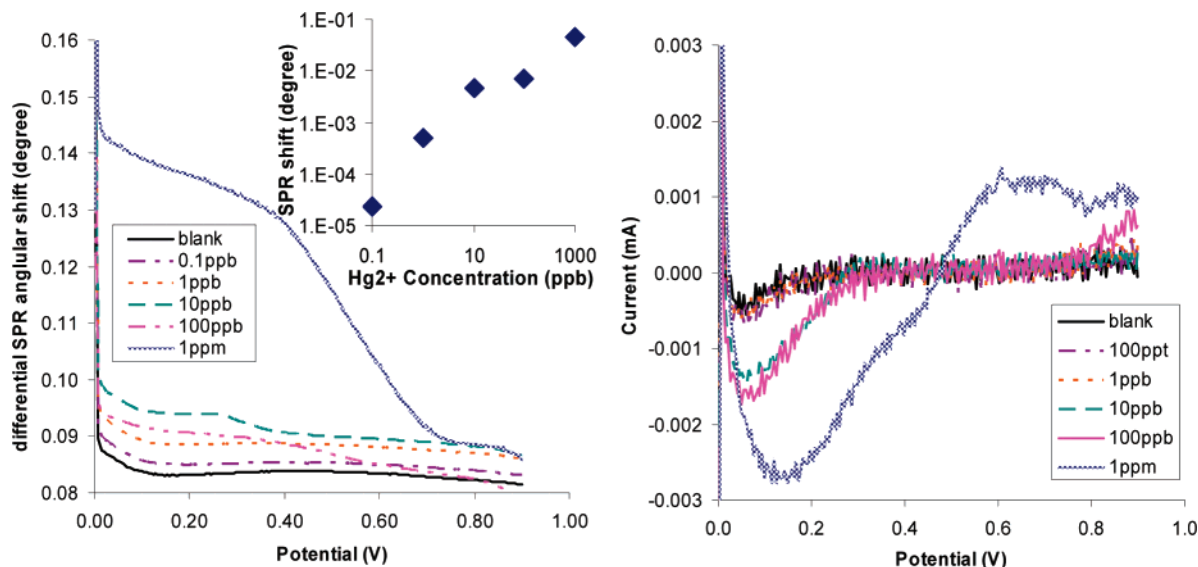


Figure 5. Quadrant cell SPR-ASV detection of different concentrations of Hg^{2+} in 100 mM HClO_4 , with 300 s of plating time at 0 V. Flow rate: 0.2 mL/min. Scan rate: 50 mV/s. Left: differential SPR signal. Right: differential current signal. Left inset: SPR shift vs Hg^{2+} concentration. The SPR angular shift is the difference in the SPR angles measured at 0.2 and 0.8 V.

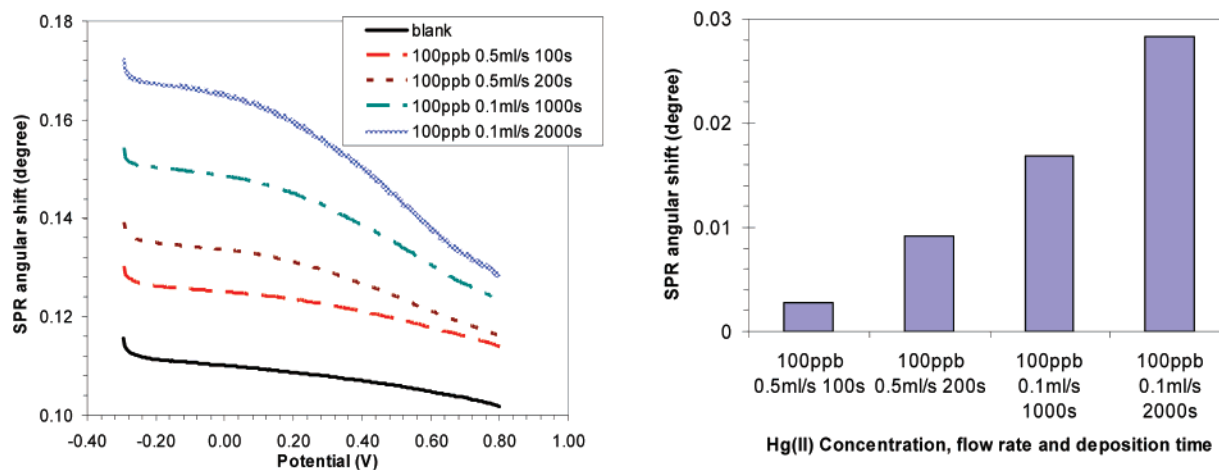


Figure 6. Influence of flow rate and plating time on mercury sensing. Flow rates were 0.5 mL/s and 0.1 mL/s, and plating times are indicated in the legend. Left: SPR vs potential. Right: net SPR shift between -0.2 and 0.8 V at different conditions.

to the applied potential and gives a flat background in the SPR angle versus potential plot in the absence of metal plating and stripping (Figure 2A). The charge density-induced SPR shift requires a large dynamic range to cover the SPR signal. To maintain the large dynamic range, the gain on the amplifier circuit has to be limited. Therefore, our quadrant cell SPR system did not show a significant sensitivity improvement over the bicell system. However, because of the introduction of the reference channel in the quadrant cell SPR system, subtraction of the reference channel is performed in real time; thus, the quadrant cell system only needs one scan to detect the sample. This advantage eases the detection and improves the efficiency of the instrument.

Background Current on SPR. The current signal in ASV typically shows multiple peaks in the background current, due to effects such as oxygen reduction and oxidation and hydrogen evolution. Oxygen can dissolve in aqueous solutions in concentrations as high as 10^{-3} M at room temperature and atmospheric pressure. Dissolved oxygen interferes with the stripping analysis as a background current. Depending upon the pH, oxygen

undergoes two-step reduction reactions.¹ The half-wave potentials of these steps are approximately -0.05 and -0.9 V versus the saturated calomel electrode (SCE). These reduction steps result in an increased background current that obscures the stripping peaks of interest. Therefore, in most of the ASV measurements, oxygen needs to be removed from the solution, though the exclusion of oxygen could be difficult for field or online operation. On the contrary, because SPR is only sensitive to the refractive index changes near the surface, the reduction of oxygen in solution will not affect the SPR signal, and thus, no oxygen removal step is required, which is an important advantage of SPR over ASV measurement.

For the same reason, hydrogen evolution does not affect the SPR signal as well. For the simultaneous detection of lead(II) and copper(II), it has been reported²⁴ that a negative stripping peak in cyclic voltammograms is shown up next to the lead stripping peak due to the hydrogen evolution that takes place on the freshly exposed copper after lead was preferentially oxidized. Our SPR signal (Figure 4) did not show any hydrogen peak, because the SPR is surface sensitive and the produced hydrogen is likely

quickly released from the surface and does not contribute to the SPR signal.

Comparison of SPR–ASV Performance with that of ASV.

The detection limit of the state-of-the-art commercial portable ASV detection system, such as the NanoBand Explorer portable metal detection system from TraceDetect, has a practical detection limit for mercury at about 2 ppb. The system uses a large volume of sample (in a beaker) with stirring. Because of the different sampling methods (flow vs static and the large difference in sampling volume), a fair comparison between the two systems is difficult. Nevertheless, our SPR system shows sub-part-per-billion detection limits for mercury that outperforms the ASV-based techniques.

CONCLUSIONS

We have demonstrated the detection of metal ions in aqueous solution using differential SPR combined with ASV. Our system demonstrated detection of lead, copper, and mercury from part-per-million down to sub-part-per-billion levels and outperformed the state-of-the-art portable electrochemistry detection system. In comparison to ASV, the SPR signal is immune to background

current, and no oxygen removal step is required. In addition, the tiny effective sampling area required by SPR makes a very compact and arrayed sensor feasible. The SPR-based detection also uses a mercury-free gold electrode, which is environmentally friendly as opposed to the typical mercury-coated electrode in ASV. The system can also be developed into a portable system for field sensing application.

ACKNOWLEDGMENT

Financial support from NSF (DMI-0214696) and DOE (DE-FG02-04ER84022) is acknowledged. S.W. thanks Dean Feaken from Nomadics Inc. for building the SPR signal amplifiers.

SUPPORTING INFORMATION AVAILABLE

Figures S-1–S-3. This material is available free of charge via the Internet at <http://pubs.acs.org>.

Received for review November 17, 2006. Accepted April 8, 2007.

AC0621773